Available online at www.sciencedirect.com
SCIENCE DIRECT®
Journal of Photochemistry and Photobiology B: Biology 79 (2005) 67–78
Journal of Photochemistry and Photobiology B:Biology
www.elsevier.com/locate/jphotobiol

Ultrafast surface solvation dynamics and functionality of an enzyme α-chymotrypsin upon interfacial binding to a cationic micelle

Rupa Sarkar, Manoranjan Ghosh, Ajay Kumar Shaw, Samir Kumar Pal *

C.K. Majumdar Laboratory, S.N. Bose National Centre for Basic Sciences, Block JD, Sector III, Salt Lake, Kolkata 700 098, India

Received 30 October 2004; received in revised form 2 December 2004; accepted 6 December 2004

Abstract

In this contribution we report studies on enzymatic activity of α-chymotrypsin (CHT) upon complexation with cationic cetyltrimethylammonium bromide (CTAB) micelle. With picosecond time resolution, we examined solvation dynamics at the interface of CHT–micelle complex, and rigidity of the binding. We have used 5-(dimethyl amino) naphthalene-1-sulfonyl chloride (dansyl chloride; DC) that is covalently attached to the enzyme at the surface sites. The solvation processes at the surface of CHT in buffer solution are found to be mostly in the sub-50 ps time scale. However, at the interface the solvation correlation function decays with time constant 150 ps (65%) and 500 ps (35%), which is significantly different from those found at the enzyme and micellar surfaces. The binding structure of the enzyme–micelle complex was examined by local orientational motion of the probe DC and compared with the case without micelle. The orientational dynamics of the probe DC in the complex reveals a structural perturbation at the surface sites of CHT upon complexation, consistent with other reported structural studies. We also found possible entanglement of charge transfer dynamics of the probe DC on the measured solvation processes by using time-resolved area normalized emission spectroscopic technique. The interfacial solvation process and complex rigidity elucidate the strong recognition mechanism between CHT and the micelle, which is important to understand the biological function of CHT upon complexation with the micelle.

Keywords: CTAB micelle; Dansyl chloride; Solvation dynamics; α-Chymotrypsin

1. Introduction

The dynamics of protein molecules is crucial for their function. Proteins in living systems are not isolated, but operating in networks and in a *carefully regulated environment*. Hydration/solvation and viscosity are among the salient properties of the environment. The fundamental role of water (hydration) for protein function and for the formation of the three dimensional structure of proteins is well-recognized and has been reviewed by several authors [1–9]. In one of these reviews [3] the role of hydration and solvent viscosity in the ability of binding carbon monoxide to wild-type and sperm whale myoglobin over a broad range of temperatures was discussed in detail. Recently, in a series of publications [10–14] followed a review [15] from Zewail's group, the time scales of the ultrafast hydration dynamics of proteins [10,11,14] and DNA [12,13] and their importance in the function of biological recognition were explored.

Numerous studies on the behavior of water-soluble and membrane enzymes in systems with low water content (reverse micelle or enzyme suspended in nonpolar organic solvents) were reviewed [16]. In the low water systems, it has been possible to probe the relation between solvation and enzyme kinetics (function), as well as some of the factors that affect enzyme thermostability and catalysis. However, the study to probe the effect of solvent on the enzymatic activity requires persistence of

* Corresponding author. Tel.: +91 33 2335 5707; fax: +91 33 2335 3477.
E-mail address: skpal@bose.res.in (S.K. Pal).

1011-1344/$ - see front matter © 2004 Elsevier B.V. All rights reserved.
doi:10.1016/j.jphotobiol.2004.12.001

structural integrity of the enzyme in the environment. Some of the experimental methods commonly used in *Micellar Enzymology* [17] give unique opportunity to study micelle-bound enzymes (in low water environment) which have minimum perturbation in the structure compared to that in physiological condition. In a recent study [18] we found that the rates of catalytic reactions of an enzyme α-chymotrypsin (CHT) included in reverse micelles with various pool sizes are retarded by, at least, two orders of magnitude compared to that in bulk water (buffer). In this way, we examined the effects of the degree of hydration on the functionality of the enzyme, since the structure were found to be almost unperturbed for all micelle-included enzymes.

Here we present our studies on the picosecond-resolved solvation dynamics at the surface of an enzyme bovine pancreatic CHT in free buffer and that of its complex with a cationic cetyltrimethylammonium bromide (CTAB) micelle. CHT is in a class of digestive enzymes of molecular weight 25 kD and has the biological function of hydrolyzing polypeptide chains. However, physiological activity is determined by the pH of the host medium [19]. The CHT–micelle complex is important to mimic the possible influence of *crowding* [20,21] or confinement of the enzyme in its *real* physiological working environment. Extensive studies [22] of the CHT–micelle complex indicate that interfacial binding interaction to the CTAB micelle increases the activity of the enzyme by a factor of 2.5 (at 20 mM CTAB concentration) compared to that in bulk water (buffer). The study concluded that the higher catalytic activity results from significant conformational change of the micelle-bound enzyme.

In this study, we have used dansyl chromophore (DC) [23] covalently attached to CHT. This labeling is well known [10,23,24] to occur mostly at ε-amino groups of the lysine and arginine residues exposed at the enzyme surface within the overall structural integrity of the enzyme. There are 10 such sites in CHT, as depicted by stick-model in Fig. 1(upper). Early studies [25,26] on the covalent attachment of the dansyl probe to CHT found that there is a certain possibility of sulfonation of the active site of the enzyme. In such cases, one *cannot* expect *functional intactness* upon the labeling of the DC to the enzyme. Here the enzymatic activity of CHT upon adduction with the dansyl probe has *not* been done. The DC undergoes a twisted intramolecular charge transfer (CT) in the excited state to generate the fluorescing state [24,27], and the process of solvation leads to continuous red shift of the emission spectrum. These dynamics are also determined by solvent relaxation [24].

We recently studied [28] the solvation and local rigidity dynamics of the stern layer of CTAB micelle by using DC as fluorescent probe. The study explored important time scale of environmental relaxation at the surface of the micelle, which was found to be important for efficient complexation with CHT. Our present studies and the study reported previously [28] from our group, use time-resolved area normalized emission (TRANES) of DC, in order to check the emission from the CT state of the probe DC during the process of solvation. By observing the picosecond to nanosecond dynamics of population and polarization analyzed anisotropy for the enzyme–micelle complex, we elucidate the nature of local solvation and polarity at the surface of CHT and binding structure of the complex.

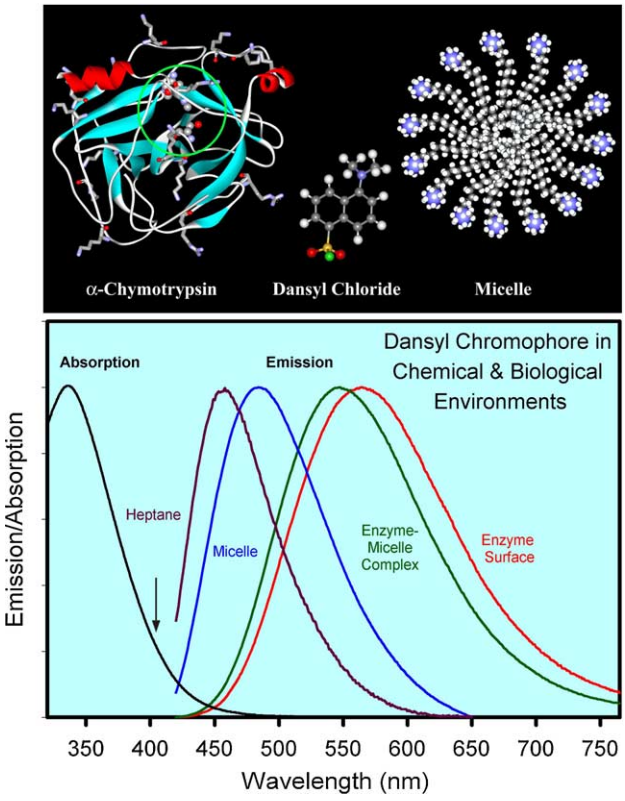

Fig. 1. (Upper) High-resolution X-ray structure of the enzyme CHT. This structure was downloaded from the Protein Data Bank (ID code 2CHA) and processed with WEBLAB-VIEWERLITE. Ten potential sites for the binding of the probe DC (lysine and arginine residues) are shown by *stick* model. Green circle shows the catalytic center (active site) of the enzyme. (Middle) Molecular structure of the probe DC is shown. (Right) A schematic of cationic CTAB micelle structure. (Lower) The normalized steady state fluorescence spectra of the probe dansyl in chemical and biological environments. Note the huge solvatochromic shift in emission. The absorption spectrum of DC bonded CHT is also shown (black line); the arrow indicates excitation wavelength (400 nm).

2. Materials and methods

The protein CHT from bovine pancreas and the substrate Ala–Ala–Phe–7-amido-4-methyl-coumarin (AMC) were purchased from Sigma, DC from Molecular Probes and CTAB from Fluka. All samples were used as received without further purifications. All the

aqueous solutions used in this study were prepared in phosphate buffer (0.1 M, pH 7).

The covalent attachment of DC to CHT (adduct formation) was achieved following the procedure from Molecular Probes. Briefly, DC was first dissolved in a small amount of dimethyl formamide and then injected into the sodium bicarbonate solution (0.1 M) of CHT (pH 8.3). The reaction was terminated by adding a small amount of freshly prepared hydroxylamine (1.5 M, pH 8.5) after incubating it for 1 h at 4–8 °C with continuous stirring. The solution was then dialyzed exhaustively against phosphate buffer (0.1 M) to separate adducts (DC–CHT) from any unreacted DC and its hydrolysis product. It should be noted that DC–CHT complexes (CHT:DC = 1.7:1) are quantitatively formed because of covalent synthesis. The enzyme concentration is maintained higher than that of the probe DC in order to avoid spatial heterogeneity in the location of the probe DC. The DC labeled CHT–micelle complexes were prepared by mixing of CTAB (50 mM) with tagged CHT (250 μM) in a neutral buffer solution.

Steady-state absorption and emission were measured with Shimadzu Model UV-2450 spectrophotometer and Jobin Yvon Model Fluoromax-3 fluorimeter, respectively. All transients were taken by using picosecond-resolved time correlated single photon counting (TCSPC) technique. In our studies we used two different setups both having commercially available picosecond diode laser pumped time-resolved fluorescence spectrophotometer from IBH, UK with different instrumental time resolution. For the dansyl-bonded CHT study we used the TCSPC setup with instrument response function (IRF) ~120 ps at Indian Institute of Technology, Kharagpur, India. The dansyl-bonded CHT–micelle complex was studied using the TCSPC setup with IRF of ~220 ps at Indian Institute of Technology, Bombay, India. The picosecond excitation pulse from the diode laser was used at 405 nm. Liquid scatterers were used to measure the FWHM of the IRF. The fluorescence from the sample was detected by a photomultiplier after dispersion through a double grating monochromator. For all transients the polarizer in the emission side was adjusted to be at 54.7° (magic angle) with respect to the polarization axis of excitation beam.

Activity measurements of CHT in the CTAB micelle were performed using AMC as the substrate. Concentration of the substrate in aqueous buffer was estimated on taking extinction coefficient value at 325 nm (ε_{350}) to be 15.9 $mM^{-1}\,cm^{-1}$. The enzyme cleaves the substrate and produces a free coumarin derivative. The absorbance of the coumarin derivative was monitored in the spectrophotometer. A cell of 1-cm path length was used for measurements both in aqueous buffer (pH 7.0) and the micelle. The enzyme concentration was 1.0 μM. The micelle-bound enzyme–substrate reactions were started by the addition of an aliquot of the stock aqueous buffered substrate solution to the pre-equilibrated micelle–CHT complex in buffer solution at 25 °C. The initial concentration of AMC was maintained in excess to that of the enzyme and was varied over a wide range. The increase in absorption at 370 nm due to the release of 7-amido-4-methyl-coumarin (in the micellar solution the extinction coefficient of the product at 370 nm was measured to be $\varepsilon_{370} = 13.4\ mM^{-1}\,cm^{-1}$) was followed [18] as time progresses. Note here that the substrate does not absorb at this monitoring wavelength. Initial rates were measured in the regime where the absorbance varies *linearly* with time. The reaction followed the Michaelis–Menten kinetics [29]. The apparent K_m and k_{cat} values were derived by least squares fitting of the double reciprocal Lineweaver–Burk plot (see below).

For anisotropy measurements emission polarization was adjusted to be parallel or perpendicular to that of the excitation and define anisotropy as $r(t) = [I_{para} - G \cdot I_{perp}]/[I_{para} + 2 \cdot G \cdot I_{perp}]$. The magnitude of G, the grating factor of the emission monochromator of the TCSPC system was found by using a coumarin dye in methanol and following longtime tail matching technique [30] to be 2.1. The steady-state anisotropy (r) was measured by using the automatic option of the fluorimeter. To construct time-resolved emission spectra after the excitation pulse, we adopted the method of [31]. For every sample solution, the fluorescence transients were measured as a function of detection wavelength in the range of 450–720 nm. The observed fluorescence transients were fitted by using a nonlinear least squares fitting procedure (software SCIENTIST) to a function comprising of the convolution of the instrument response function with a sum of exponentials. The purpose of this fitting is to obtain the decays in an analytic form suitable for further data analysis. For each detection wavelength, the transient was normalized by using the steady-state spectrum. The resulting time-resolved spectra were fitted with a Lognormal shape function to estimate the spectrum maximum $\nu(t)$. The temporal Stokes shift can be represented by the time dependence of the fit. By following the time-resolved emission, we constructed the solvation correlation function, $C(t) = [\nu(t) - \nu(\infty)]/[\nu(0) - \nu(\infty)]$, where $\nu(0)$, $\nu(t)$ and $\nu(\infty)$, denote the observed emission energies (in wavenumbers) at time 0, t and ∞, respectively. For the construction of TRANES spectra we followed methods as described in [32].

3. Results and discussion

3.1. Steady-state spectroscopic studies

Fig. 1(lower) shows emission spectra of the DC in various environments. At the surface of the enzyme CHT dansyl (covalently bound) shows a fluorescence

peak at 564 nm. When dansyl-bonded enzyme made complex with CTAB micelle, the emission maximum shifts to 547 nm. The blue shift of the chromophore emission in the micelle-bound CHT compared to that in the free enzyme clearly indicates a significant portion of the CHT surface is involved in the complexation. The fluorescence spectrum of the dansyl probe with the CTAB micelle peaks at 484 nm. For all cases (except for DC in *n*-heptane) the excitation wavelength was maintained at 400 nm, as indicated by an arrow in the absorption spectrum of the DC bonded CHT sample. The emission spectrum of DC in bulk *n*-heptane, a non-polar solvent is also shown for comparison: the fluorescence has maximum at 457 nm (excitation at 350 nm), which is 110 nm blue shifted compared to that at enzyme surface. From the steady-state spectra, the solvatochromic shift of the fluorescence towards longer wavelengths with increasing environmental polarity is evident. Significantly large polarity dependent solvatochromic red shift makes DC an attractive probe for hydration/solvation dynamics of microenvironments of biological macromolecules [10,24]. A detail molecular picture of solvation for the probe DC has been given in [24].

3.2. Enzymatic activity measurements

Fig. 2(upper) shows time dependent product concentration as a result of enzymatic activity of CHT in CTAB micellar environment ([CTAB] = 50 mM, pH 7.0). For comparison we also show the enzymatic behavior in free buffer (pH 7.0). For both the cases the enzyme and substrate concentrations were maintained to be 1 and 334 μM, respectively. Fig. 2(lower) depicts the Lineweaver–Burk plot, where the reciprocal of the reaction velocity (v) is plotted as a function of the reciprocal of the initial concentration of AMC in the aqueous buffer solution. The linear behavior is appropriate because the kinetics is in the Michaelis–Menten regime where the concentration of the substrate is much higher than that of the enzyme CHT ([E]). This allows one to obtain the dissociation and rate constants, (K_m) and k_{cat}, respectively. From the slope (K_m/v_{max}; v_{max} is the maximum velocity) and intercept ($1/v_{max}$) of the numerical fitting. The values of K_m and k_{cat} ($v_{max}/[E]$) were found to be 0.38 mM and 0.1 s^{-1}, respectively.

We would like to mention here that our earlier studies [18] of enzyme–substrate kinetics involving the same substrate (AMC) in free buffer (pH 7.0) reported that the values of K_m and k_{cat} were 2.5 mM and 4.9 s^{-1}, respectively. Present work indicates that the micelle-bound CHT presents 7 times lower catalytic efficiency (k_{cat}/K_m) than the free enzyme. Recent studies [22] of micelle-bound enzyme–substrate kinetics involving the substrate *p*-nitrophenyl acetate (PNPA) reported the values of K_m and k_{cat} to be 29.7 μM and 101 s^{-1}, respectively, in presence of 20 mM CTAB. It was also found

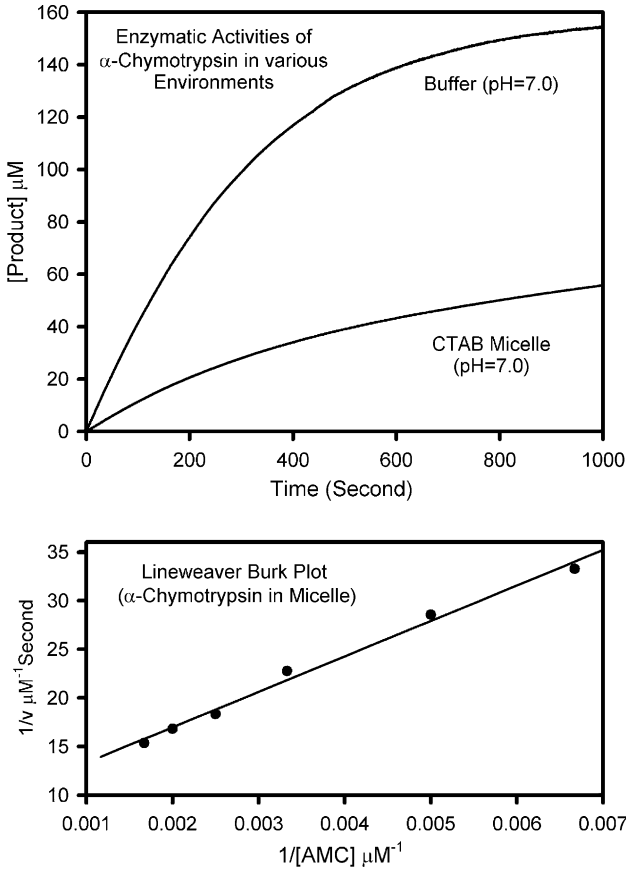

Fig. 2. (Upper) Comparison of the activity of the enzyme CHT in free buffer with that in micellar solution. The rate of product formation in *aqueous buffer* is slower than that in *micellar solution* (see text). For both the samples enzyme and initial substrate concentrations were maintained at 1 and 150 μM, respectively. (Lower) Lineweaver–Burk plot of the enzyme CHT showing its catalytic activity with substrate AMC in the micellar solution at pH 7.0. The solid line is a linear fit following Michaelis–Menten kinetics.

that the micelle-bound enzyme had 2.5 times higher catalytic efficiency than that of the free enzyme in buffer. However, the study confirmed decrease in enzymatic activity with higher (more than 20 mM) CTAB concentrations and concluded to be due to unfavorable partition of the substrate into the micelle.

In contrast, another study involving a substrate *N*-glutaryl-L-phenylalanine *p*-nitroaniline [33] found an opposite effect with CTAB micelle where 20% decrease on the original CHT (in free buffer), which is qualitatively in agreement with our observation. Recently theoretical models were developed [34] for the treatment of reaction rates of an enzyme in the micellar environments. These models consider both the partitioning of the substrate and the ion exchange at the micellar interface. Three pseudophases: free water, water bound at the micellar surface and that in the micellar core have also been considered in these models. The models predict that the reaction rate of the enzyme exhibits a bell-shaped dependence of surfactant concentration

when enzyme–micelle interactions are included in the formulation of the model. The bell-shaped dependence of reaction rate of CHT on CTAB concentration is recently found in the literature [22].

3.3. Location of the substrate and product

The interaction of the substrate with the micellar surface, which leads to partitioning of the substrate into aqueous and micellar phases [22,34] is important points to understand the activity of micelle-bound CHT. A significant affinity of the substrate to the micellar surface essentially decreases the activity of the enzyme CHT with higher CTAB surfactant concentration (above CMC) due to unfavorable partitioning of the substrate into micelle [22]. On the other hand, for optimum activity of a micelle-bound enzyme, the product must have minimum affinity to the micellar surface in order to create space for the substrate by leaving the active site of the enzyme at the micellar surface. Thus it is important to know the immediate environments of the free substrate and product in the micellar solution in absence of the enzyme. In Fig. 3 we show dependence of emission intensities of the substrate (upper) and product (lower) on the concentration of the surfactant (CTAB). We further compare intensities of the probes (substrate and product) in solvents (water–ethanol mixture) with different polarities without micelle. Inset figures show changes of relative intensities of the probes in water–ethanol mixture with various ethanol concentrations. The shifts of the maxima of emission spectra of the substrate and product were found to be very small (3–5 nm) toward blue wavelength upon decreasing the polarity of the mixture solution by adding more ethanol (from 0% to 100%). Hence, the solvatochromism and intensity change of the substrate and the product are *not* good probes for their local environmental information.

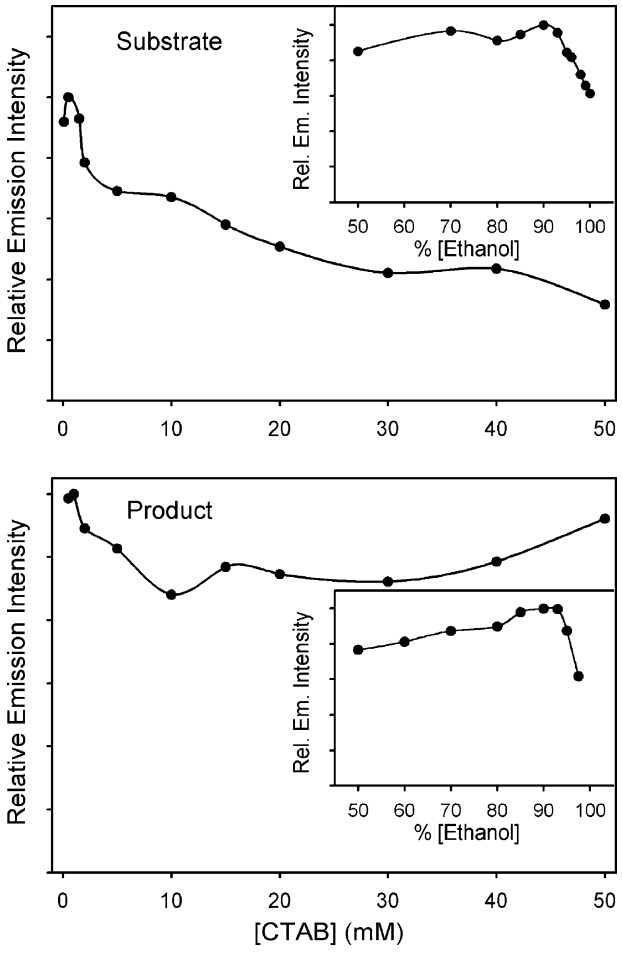

Fig. 3. Dependence of emission intensities of the substrate (upper) and product (lower) on the concentration of the surfactant (CTAB). Insets show changes of relative intensities of the probes (substrate and product) in water–ethanol mixture with various ethanol concentrations.

However, the steady-state anisotropy studies of the substrate and product give some information about their locations in the micellar solutions as evidenced from Fig. 4. The measured steady-state anisotropy value for the substrate in aqueous 50 mM CTAB solution is higher ($r = 0.08$) than that of the product ($r = 0.02$) indicating stronger favorable interaction of the substrate with the micelle compared to that of the product. The critical micellar concentration (CMC) of CTAB in the buffer (0.1 M phosphate) was measured by using a fluorescent laser dye DCM (data not shown) and found to be ~0.8 mM. For comparison the anisotropy values of the substrate (upper panel) and product (middle panel) in free buffer were also shown. We found a small difference between the anisotropy values of substrate and product in free buffer. Relatively higher anisotropy of the product in the micellar solution (middle panel) compared to that in free buffer indicates an attractive interaction of the product with the micelle. As the emission peaks of the substrate (390 nm) and product (440 nm) are well separated, in a substrate–product mixture solution a long-range wavelength scanning of steady-state anisotropy is expected to show the signature of both solutes in the solution, which is clearly evident from the lower panel of Fig. 4.

From the earlier report it was evident that CTAB micelle-bound CHT had tendency to react with the free substrate in the aqueous phase [22] rather reacting with micelle-bound substrate. The affinity of the micelle-bound CHT is similar to that of a matrix enzyme [35]. The observed decrease in activity in our experiment, which is in contrast with the superactivity found in the study [22] can be explained by the unfavorable partitioning of the substrate for its affinity to the micelle and/or finite attractive interaction of the product to the micellar environment as evidenced from the anisotropy study.

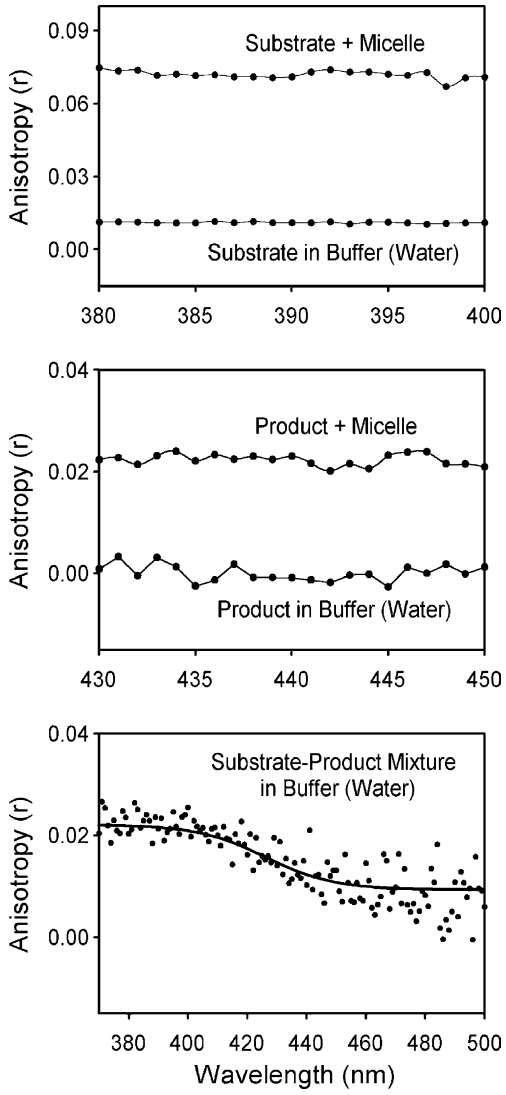

Fig. 4. Steady-state anisotropies of the substrate (upper) and the product (middle) in free buffer and in micellar solution. Lower panel shows steady-state anisotropy of the mixture of substrate and product in free buffer (see text).

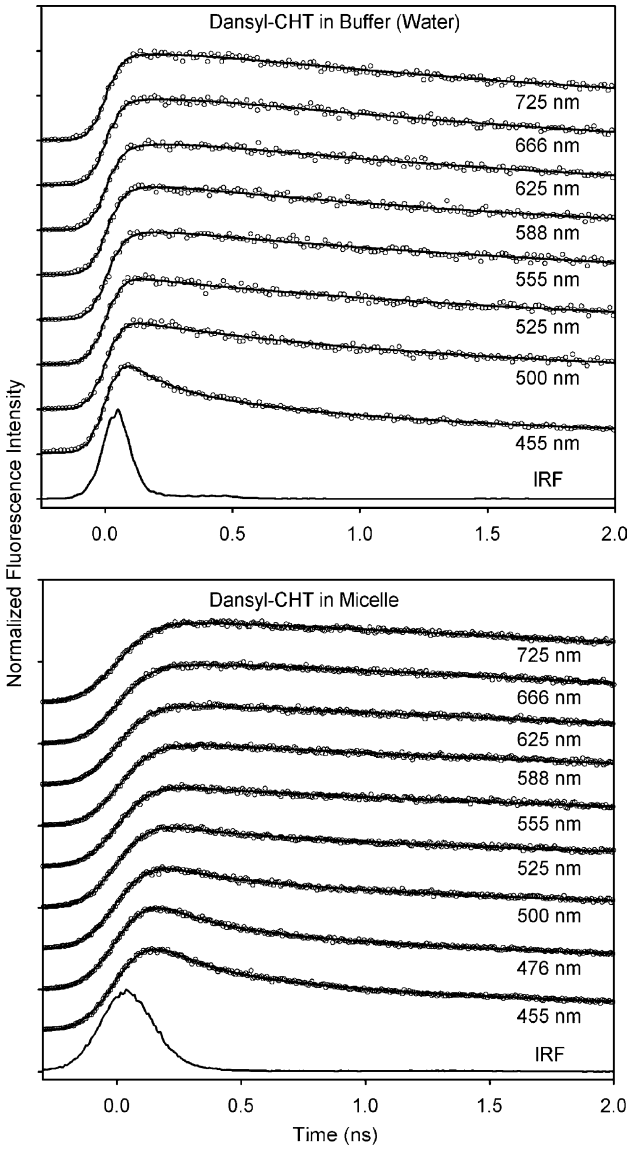

Fig. 5. Picosecond-resolved transients of the DC–CHT adduct (upper) and DC labeled CHT–micelle complex (lower). Instrument response functions (IRF) for both the set of transients are shown. The transients are normalized and baseline shifted for comparison.

3.4. Time-resolved studies

3.4.1. Dansyl-bonded CHT in free buffer: dynamics of solvation

Fig. 5(upper) shows the picosecond-resolved transients of DC attached to CHT with a series of systematic wavelength detection. The signal initially decays with time constant 150 ps at the blue side of fluorescence but rises with similar time constant at red side. Two decay components for all wavelengths were found with a time constant of ~2 and 8 ns as shown in Fig. 5(upper). The observed decay component (2 ns) could be due to CT dynamics [24,27] at the protein surface. The slower 8 ns component is the fluorescence lifetime of the probe DC in the protein environment. Note that at the micellar surface (relatively nonpolar) DC shows fluorescence lifetime of 12 ns and complete absence of the 2 ns decay component [28].

The constructed time-resolved emission spectra (TRES) are shown in Fig. 6(upper). The steady-state spectrum of DC–CHT adduct is also shown for comparison (dotted line). The solvation correlation function $C(t)$ (Fig. 6(lower)) shows single exponential decay with time constant of 142 ps; any sub-50 ps components in these dynamics are unresolved. The net spectral shift ($\Delta\nu$) is 74 cm^{-1} from 17,064 to 16,990 (up to 700 ps). Note that for DC at the micellar surface [28] we recovered $\Delta\nu$ to be 374 cm^{-1} from 20,441 to 20,067 cm^{-1} (up to 2 ns). For DC bonded CHT–micelle complex the values of $\nu(0)$ and $\Delta\nu$ are found to be 19,397 and

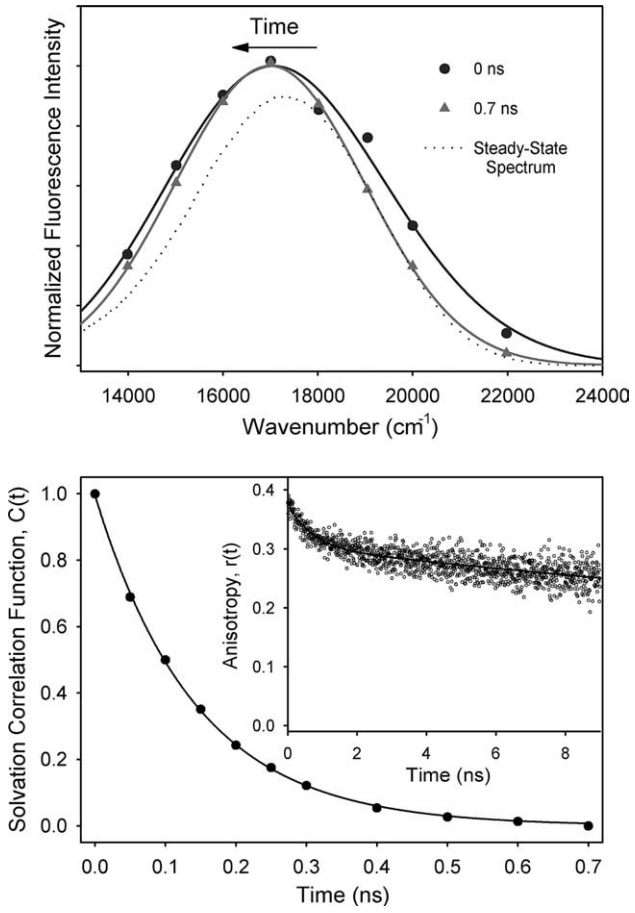

Fig. 6. (Upper) Time-resolved emission spectra (TRES) of the probe DC at the enzyme surface. Steady-state spectrum of the sample is also shown for comparison (dotted line). (Lower) Solvation correlation function, $C(t)$, of DC at the enzyme surface. Insets shows the time-resolved anisotropy, $r(t)$, of DC in the same system.

1068 cm^{-1}, respectively (see below). The smaller magnitude of $\Delta\nu$ and significantly large red shifted $\nu(0)$ for DC labeled CHT in buffer compared to those either at the micellar surface [28] or in the CHT–micelle interface, clearly indicates a considerably large *missing* dynamics in our observed $C(t)$ decay. This is not surprising given that time scale of dynamics (hydration) at the surface of proteins in buffer is 20–40 ps ([15] and references therein), which is beyond our experimental resolution. However, our observations are complimentary to those studies with femtosecond resolution.

The anisotropy $r(t)$ of DC attached to CHT is shown in the inset of Fig. 6(lower). The measured $r(t)$ decays with time constants 690 ps (20%) and ~47 ns (80%) resulting a persistency of $r(t)$ in our experimental window (up to 10 ns). The value of $r(t)$ at $t = 0$ is found to be 0.38. The dynamics of $r(t)$ which corresponds to the structural relaxation of the probe DC at the protein surface is drastically different from that in bulk methanol, observed with femtosecond resolution [24]. In methanol, the two major components of $r(t)$ decay have time constants 14 ps (40%) and 50 ps (50%), except for small initial decay (10%) which corresponds to the structural relaxation from ultrafast solvation. However, at the micellar surface [28] DC probe shows different dynamics of $r(t)$. The decay of $r(t)$ almost merges exponentially the baseline in 5 ns experimental window with time constants of 413 ps (23%) and 1.3 ns (77%). When DC is covalently connected to CHT, the huge residual anisotropy up to 10 ns indicates restriction of the orientational relaxation due to the anchoring at the protein surface.

3.4.2. Enzyme–micelle complex

Fig. 5(lower) shows picosecond-resolved transients of the DC bonded CHT–micelle complex in aqueous buffer solution. On the blue edge of the fluorescence spectrum the signals decay with time constants (150–250 ps) depending on wavelengths, whereas on the red edge the signals are seen to rise (time constant up to 1.0 ns). A decay component of time constants ~2 ns and a relatively long ~12 ns decay component reflective of lifetime of the probe are present in all wavelengths detected (Fig. 5(lower)). Fig. 7(upper) shows TRES (up to 2.4 ns) of the complex in aqueous buffer. The dotted spectrum indicates the steady-state spectrum of the complex. It is evident that equilibrium (steady-state) spectrum requires further time to reach, consistent with the longer time scale for post-solvated activated CT in DC [24].

The $C(t)$ function in Fig. 7(lower) can be fitted to a biexponential decay with time constants of 150 ps (65%) and 500 ps (35%); any sub-50 ps components in these dynamics are unresolved. The net spectral shift is 1068 cm^{-1}; from 19,397 to 18,329 cm^{-1} (up to 2.4 ns). The shift is much larger than that of the CHT without micelle, indicating significantly smaller *missing* dynamics with our experimental resolution. The faster time constant of 150 ps is similar to the solvation time 142 ps of CHT without micelle, reflective of the probe environments and not that of the CHT–micelle interface. However, longer time constant of 500 ps (35%) is considerably slower than that of either CHT in bulk buffer (142 ps) or micellar surface (374 ps), indicative of an environment at the interface between CHT and the micelle.

As shown in the inset of Fig. 7(lower) the fluorescence anisotropy $r(t)$ at 555 nm decays exponentially to almost baseline with time constants of 1.2 ns (40%) and 8.5 ns (60%). In contrast to the enzyme without micelle the anisotropy at $t = 0$ (0.3) and significantly small residual anisotropy (up to 10 ns) reveal faster rotational dynamics of the probe DC upon complexation with the micelle. The change in the dynamics is consistent with the perturbation of surface structure of the enzyme (CHT) upon complexation with the CTAB micelle, as evidenced from other studies using circular dichroism and FT-IR spectroscopy [22].

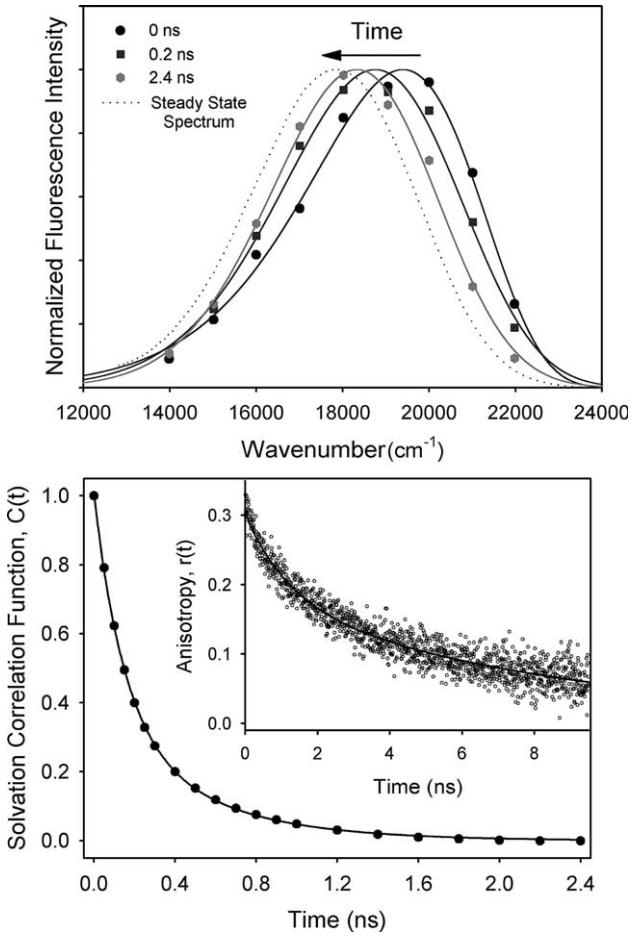

Fig. 7. (Upper) Time-resolved emission spectra (TRES) of the probe DC in the enzyme–micelle complex. Steady-state spectrum of the sample is also shown for comparison (dotted line). (Lower) Solvation correlation function, $C(t)$, of DC in the enzyme–micelle complex. Inset shows the time-resolved anisotropy, $r(t)$, of DC in the same system.

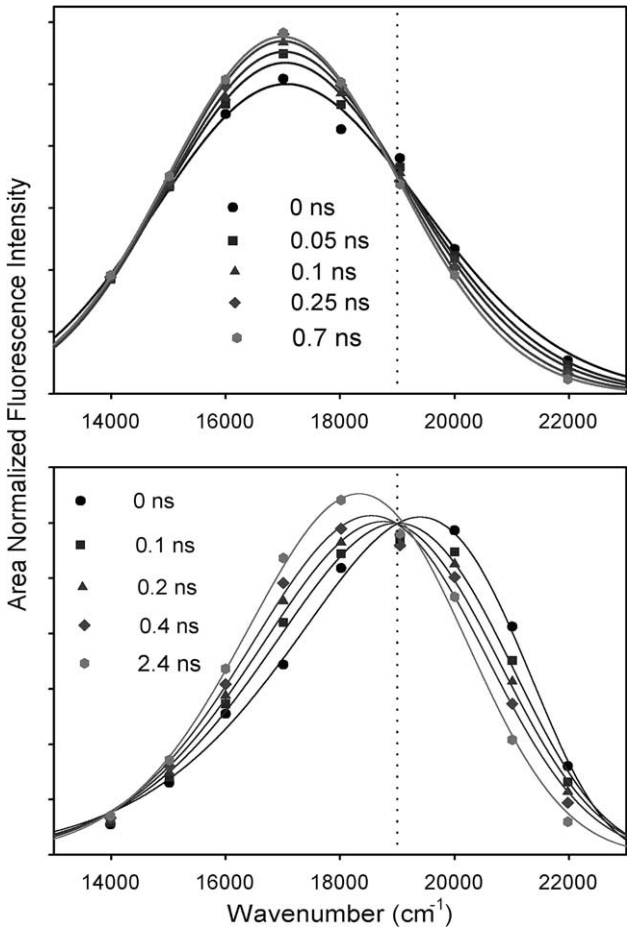

Fig. 8. Time-resolved area normalized spectra (TRANES) of DC at enzyme surface (upper) and in the enzyme–micelle complex (lower). Note the isoemissive points at 19,000 cm^{-1} for both the systems (see text).

3.4.3. Existence of two species

As mentioned in the previous sections, a decay component of time constant of 2 ns is present in all detected transients (Fig. 5) for DC–CHT in free buffer and with the micelle. The decay of similar time constant (2 ns) for both the samples we studied could be a manifestation of existence of excited state twisted CT state. To ascertain possible entanglement of emission from two states (locally excited (LE) and CT states) we further use TRANES technique, which has been developed recently [32]. As described in [32] TRANES is a model free modified version of TRES mentioned above. Fig. 8 shows TRANES spectra of DC attached to CHT without (upper) and with micelle (lower). An isoemissive point at 19,000 cm^{-1} is clearly evident in the spectra of both the samples. One of the possible reasons of existence of two emissive species in the excited state is due to the solubilization of the DC in two different sites of the micelle [32]. However, our observation of entanglement of conformational dynamics with the solvation and other steady-state study reported in [27] support the coexistence of the excited CT state with the LE state (before CT).

3.4.4. Diffusion of the probe DC through various environments: emission line-width analysis

The full-width at half maxima (line widths; Γ) of emission spectra of the DC probe (Fig. 1(lower)) were observed to be different in various chemical and biological environments. The line width increases upon changing the polarity of the immediate environment of DC. In *n*-heptane (nonpolar), micellar surface, enzyme–micelle interface and at the surface of CHT the values of Γ were found to be 3671, 4261, 4460 and 4553 cm^{-1}, respectively. The observation is consistent with the fact that in the polar environment fluorescence spectrum of a solute (DC) with higher excited state dipole moment compared to that in ground state is the superposition of emission from different excited states of diverse degrees of solvation [31]. The broadening of emission spectrum

may also be indicative of spatial microheterogeneity of the immediate environment of the probe DC [36–38].

The line width (Γ) of TRES (Fig. 9) of DC is found to vary with time, which is an evidence of change in local environment during solvation. At the enzyme surface (Fig. 9(upper)) $\Gamma(t)$ exhibits a fast decay with time constants 60 ps (80%) and 250 ps (20%). Total change of line width ($\Delta\Gamma$) is 714 cm^{-1} (up to 700 ps; from 5439 to 4725 cm^{-1}) which is 13% of the width at $t = 0$. At the micellar surface (Fig. 9(middle)) (t) shows a single exponential decay with time constant 525 ps. The net change of $\Delta\Gamma$ is 345 cm^{-1} (up to 2 ns; from 4986 to 4641 cm^{-1}) that is 10% of the spectral line width at $t = 0$. In the case of DC at the interface between CHT and micelle, $\Gamma(t)$ exhibits a fast initial rise (time constant 90 ps) followed by biexponential decay with time constants 120 ps and 3.6 ns (Fig. 9(bottom)). The net $\Delta\Gamma$ of the rise component (up to 150 ps; from 4689 to 4880 cm^{-1}) is 191 cm^{-1}. For the decay component the net $\Delta\Gamma$ is observed to be 368 cm^{-1} (up to 2.4 ns; from 4880 to 4512 cm^{-1}).

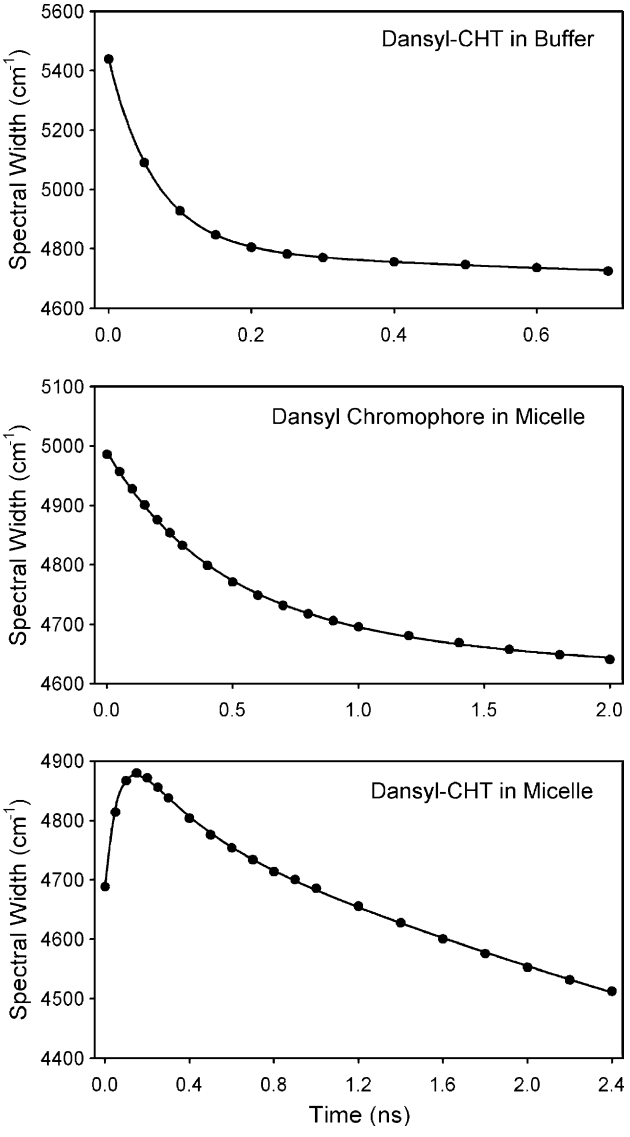

Fig. 9. Time-resolved line width (Γ) of TRES of DC at the enzyme surface (upper), DC at micellar surface (middle) and DC in the CHT–micelle complex (lower).

From the studies of time dependent spectral width an interesting feature of relaxation dynamics of DC in the enzyme–micelle interface is evident. The fast rise with time constant 90 ps is an indicative of diffusion of the probe DC from nonpolar to polar environment. The time constant is also similar to the case of DC at the surface of CHT (60 ps). Conversely, in the latter case the faster time constant of 60 ps results a decay that is an indication of polar to nonpolar diffusion. In the interface the rise–decay characteristics of Γ (t) is one of the clear indications of scanning of the interfacial environment by the probe DC. Most expectedly, the probe first diffuses from the surface of CHT (nonpolar) to the relatively polar (interface) region and then further diffuses to the vicinity of the micellar surface (nonpolar). A similar dynamical characteristics is supposed to be evidenced from the time dependence of $r(t)$. The instrumental resolution (~50 ps) is close to the time scales of the faster dynamics and could be possible cause for the missing dynamics of $r(t)$. However, the slower component of $\Gamma(t)$ (3.6 ns) is close to the faster ns component (1.2 ns) of $r(t)$ decay.

4. Activity, dynamics and energetics

Upon complexation with the CTAB micelle CHT shows hypo-activity (the study reported here) and superactivity [22] on substrates AMC and PNPA, respectively (Table 1). The overall retardation and enhancement of the enzymatic activity (k_{cat}/K_m) are estimated to be 7 and 2.5 times, respectively. The superactivity [22] of CHT has been correlated with the changes of the secondary structure (e.g. increase in the α-helix content and a decrease in the β-sheet while the turns and unordered contents remained unchanged) compared to the free enzyme in the buffer solution. However, it should be mentioned that the change in the activities in the above studies are *not* sufficient to conclude an important change in the interactions (and/or overall conformations) of micelle-bound CHT with the substrates. For example, if there is a change of stabilization energy of an enzyme–substrate complex by 4 kcal/mol which is a typical value associated with a hydrogen bonding interaction at 298 K, the effect on the rate of the enzymatic reaction changes by a factor of 288.

The enzymatic activity is shown schematically as follows:

Table 1
Kinetic parameters for the enzymatic activity of CHT with two substrates AMC and PNPA at 27 °C

Medium	K_m (μM)	k_{cat} (s^{-1})	k_{cat}/K_m ($M^{-1}\,s^{-1}$)	ΔG_s (kcal mol^{-1})
	Enzymatic hydrolysis of AMC			
Buffer	2500	4.9	1960	−3.55
Micelle	380	0.1	263	−4.66
	Enzymatic hydrolysis of PNPA			
Buffer	44	61.8	1.4×10^6	−5.94
Micelle	29.7	101.4	3.4×10^6	−6.17

The parameters for the activity with the substrate PNPA were taken from the work [22]. The free energy for enzyme–substrate complexation is $\Delta G_s = -RT \times \ln(1/K_m)$ [29].

$$\underset{\text{Entrance}}{E + S \overset{K_m}{\leftrightarrow} ES} \quad \underset{\text{Exit}}{\overset{K_{cat}}{\leftrightarrow} E + P}$$

where E, S and P indicate enzyme, substrate and product, respectively. The entrance and exit channels of the reaction are also indicated. From Table 1, it is evident that CHT–PNPA complex is energetically more stabilized than the CHT–AMC complex in absence of the micelle. As evidenced by relative change of k_{cat} values most significant cause for the retardation of the activity of CHT reported here is the destabilization of the barrier in the exit channel of the micelle-bound enzyme compared to that of the free CHT. The solvation dynamics of the micelle-bound enzyme shows two distinct time constants 150 ps (65%) and 500 ps (35%). The longer one indicates that a significant portion of the enzyme surface (~35%) is in the close vicinity of the micelle to facilitate the interfacial binding with the micelle. In a micellar environment diffusion of the product would expectedly be slower compared to that in free buffer. Slow diffusion from the catalytic site of the micelle-bound CHT and affinity of the product to the micelle that is evidenced by our steady-state anisotropy measurement expectedly *retard* the process of product dissociation from the enzyme resulting destabilization of the energy barrier in the exit channel. Another important observation is a large dynamical Stokes shift in the TRES of the complex (1068 cm^{-1}) compared to that in enzyme in free buffer (74 cm^{-1}), which reveals less amount of missing dynamics within our experimental window. In other words the time constants observed in our experiment are mostly responsible for the entire relaxation processes at the surface of the micelle-bound enzyme. The observation clearly indicates more rigid environment around the micelle-bound CHT compared to that of free enzyme in buffer. The enzymatic activity of CHT upon complexation with the micelle depends on rigidity of the environment around the enzyme and/or its structural flexibility [3]. The rigid environment in the close vicinity of the enzyme surface may retard the interaction with the substrate resulting the hypo-activity observed in our experiment.

5. Conclusion

The overall picture, which emerges from our studies, is depicted in Fig. 10. Solvation dynamics at the surface were measured from the solvent response as probed by the dynamical Stokes shift of the ligand DC during solvation. The solvation process at the surface of CHT in absence of the micelle were found to be mostly ultrafast, less than 50 ps, indicated by very small dynamical Stokes shift with time constant 142 ps. This observation is in agreement with the previous studies of femtosecond-resolved hydration dynamics at the protein surfaces [15] and is significant for the recognition of substrate and/or other protein by CHT. The surface of CHT

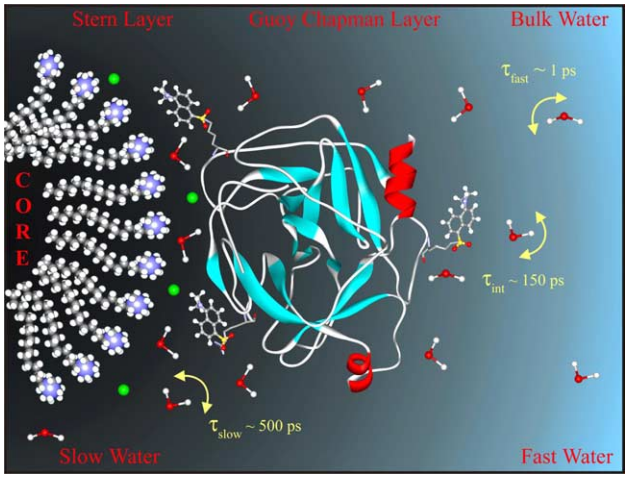

Fig. 10. Model of the interaction between the protein CHT and the CTAB micelle, showing interfacial dynamics studied through the covalent labeling of the probe DC (three possible sites were shown using ball & stick model) to the enzyme. The gradient of black color is an indication of variation of hydrophobicity/rigidity of the environments in the CHT–micelle complex. The hydrophobicity decreases gradually from its highest value in the core (black) of the micelle to the lowest one in the bulk water (blue). The distribution of solvation time in the complex defines three types of water motions: bulk water (weak interaction; ~1 ps), intermediate in the Guoy Chapman layer (~150 ps) and those much slower (strong interaction; ~500 ps) in the interface of the complex.

presumably optimize binding of substrate (or other protein/aggregate) involving efficient dehydration process by utilizing labile water, unlike slow structural water layer needed to maintain 3D structure. However, dynamical anisotropy, which probes orientational motions of the ligand DC covalently adducted at the surface of CHT persists for more than 10 ns, in contrast to the behavior at the micellar surface or in bulk methanol indicating restriction of physical motions of the probe DC at the surface of CHT.

The enzyme forms complexes with CTAB micelle [22], which is expected to be sandwich like (Fig. 10). The steady-state fluorescence also indicates the complexation of DC-bonded CHT with the micelle (Fig. 1). The solvation process of the complex, which is different from those at the enzyme and micellar surfaces, gives two distinct time constants of 150 ps (65%) and 500 ps (35%) indicating spatial heterogeneity of the local environment of the ligand DC at the interface. The time constant of 150 ps of the $C(t)$ decay is similar to the observed slower component of the solvation process at the surface of CHT without micelle. However, it is faster than that at micellar surface (340 ps). As shown in the Fig. 10, the water molecules in the relatively less rigid environments (Guoy Chapman layer) compared to stern layer of the micelle [39] could also result the faster dynamics. The slower time constant of the CHT–micelle complex (500 ps) is significantly different from those at micellar and enzyme surfaces and can be assigned to be solely due to the interfacial relaxation.

The rigidity of the micelle–enzyme complex was measured by time-resolved anisotropy, which probes orientational motions of the ligand DC covalently adducted at the surface of the enzyme. The dynamical nature of the anisotropy ($r(t)$ decay) is different from those at the enzyme and micellar surfaces, which reveals a structural perturbation as evident from other studies. TRANES analysis of the time-resolved fluorescence spectra of the samples anticipates possible entanglement of emission from the CT state dynamics in the process of solvation.

Studies of picosecond dynamics of the probe DC at the enzyme surface and in the enzyme–micelle interface elucidate nature of biomolecular recognition process and the time scales involved for complex rigidity and solvation. These studies attempt to link structural and dynamical features for insight into the biological function (activity) of the enzyme CHT in restricted (real) environments.

6. Abbreviations

DC	dansyl chloride
CHT	α-chymotrypsin
CTAB	cetyltrimethylammonium bromide
CT	charge transfer
AMC	Ala–Ala–Phe–7-amido-4-methyl-coumarin
PNPA	*p*-nitrophenyl acetate
TRES	time-resolved emission spectra
TRANES	time-resolved area normalized emission spectra

Acknowledgments

We thank Professor Sushanta Dattagupta, Director, S.N. Bose National Centre for Basic Sciences for his continued support, interest and encouragement. We thank Drs. Nilmoni Sarkar, IITKGP and Anindya Datta, IITB, India for their support and help during the time-resolved measurements. We thank Dr. Jaydeb Chakrabarti, S.N. Bose National Centre for Basic Sciences for stimulating discussions.

References

[1] A.R. Bizzarri, S. Cannistraro, Molecular dynamics of water at the protein–solvent interface, J. Phys. Chem. B 106 (2002) 6617–6633.
[2] V.P. Denisov, B. Halle, Protein hydration dynamics in aqueous solution, Faraday Discuss. 103 (1996) 227–244.
[3] H. Frauenfelder, P.W. Fenimore, B.H. McMahon, Hydration, slaving and protein function, Biophys. Chem. 98 (2002) 35–48.
[4] G. Otting, E. Liepinsh, K. Wuthrich, Protein hydration in aqueous solution, Science 254 (1991) 974–980.
[5] S.K. Pal, J. Peon, B. Bagchi, A.H. Zewail, Biological water: femtosecond dynamics of macromolecular hydration, J. Phys. Chem. B 106 (2002) 12376–12395.
[6] Y. Pocker, Water in enzyme reaction: biophysical aspects of hydration–dehydration processes, Cell. Mol. Life Sci. 57 (2000) 1008–1017.
[7] J.A. Rupley, G. Cateri, Protein hydration and function, Adv. Prot. Chem. 41 (1991) 37–172.
[8] B.P. Schoenborn, A. Garcia, R. Knott, Hydration in protein crystallography, Prog. Biophys. Mol. Biol. 64 (1995) 105–119.
[9] M. Tarek, D.J. Tobias, The dynamics of protein hydration water: a quantitative comparison of molecular dynamics simulations and neutron-scattering experiments, Biophys. J. 79 (2000) 3244–3257.
[10] S.K. Pal, J. Peon, A.H. Zewail, Biological water at the protein surface: dynamical solvation probed directly with femtosecond resolution, Proc. Natl. Acad. Sci. USA 99 (2002) 1763–1768.
[11] S.K. Pal, J. Peon, A.H. Zewail, Ultrafast surface hydration dynamics and expression of protein functionality: α-chymotrypsin, Proc. Natl. Acad. Sci. USA 99 (2002) 15297–15302.
[12] S.K. Pal, L. Zhao, T. Xia, A.H. Zewail, Site and sequence selective ultrafast hydration of DNA, Proc. Natl. Acad. Sci. USA 100 (2003) 13746–13751.
[13] S.K. Pal, L. Zhao, A.H. Zewail, Water at DNA surfaces: ultrafast dynamics in minor groove recognition, Proc. Natl. Acad. Sci. USA 100 (2003) 8113–8118.
[14] J. Peon, S.K. Pal, A.H. Zewail, Hydration at the surface of the protein Monellin: dynamics with femtosecond resolution, Proc. Natl. Acad. Sci. USA 99 (2002) 10964–10969.
[15] S.K. Pal, A.H. Zewail, Dynamics of water in biological recognition, Chem. Rev. 104 (2004) 2099–2123.
[16] M.T. de Gomez-Puyou, A. Gomez-Puyou, Enzymes in low water systems, Crit. Rev. Biochem. Mol. Biol. 33 (1998) 53–89.

[17] A.V. Levashov, N.L. Klyachko, Micellar enzymology: methodology and technique, Russ. Chem. Bull. Int. Ed. 50 (2001) 1718–1732.
[18] R. Biswas, S.K. Pal, Caging enzyme function: α-chymotrypsin in reverse micelle, Chem. Phys. Lett. 387 (2004) 221–226.
[19] D. Voet, J.G. Voet, Biochemistry, Wiley, Somerset, NJ, 1995, pp. 398–400.
[20] A.P. Minton, The influence of macromolecular crowding and macromolecular confinement on biological reactions in physiological media, J. Biol. Chem. 276 (2001) 10577–10580.
[21] A.S. Verkman, Solute and macromolecule diffusion in cellular aqueous compartments, TIBS 27 (2002) 27–33.
[22] M.S. Celej, M.G. D'Adrea, P.T. Campana, G.D. Fidelio, M.L. Bianconi, Superactivity and conformational changes on α-chymotrypsin upon interfacial binding to cationic micelles, Biochem. J. 378 (2004) 1059–1066.
[23] R.P. Haugland, Handbook of Fluorescent Probes and Research Chemicals, Molecular Probes, Eugene, OR, 1996, pp. 8–13.
[24] D. Zhong, S.K. Pal, A.H. Zewail, Femtosecond studies of protein–DNA binding and dynamics: Histone I, Chemphyschem 2 (2001) 219–227.
[25] B. Hartley, V. Massey, The active centre of chymotrypsin I. Labelling with a fluorescent dye, Biochim. Biophys. Acta 21 (1956) 58–70.
[26] R.P. Haugland, L. Stryer, A fluorescent probe at the active site of α-chymotrypsin, in: G.M. Ramachandran (Ed.), Conformation of Biopolymers, vol. I, Academic Press, New York, 1967, pp. 321–333.
[27] B. Ren, F. Gao, Z. Tong, Y. Yan, Solvent polarity scale on the fluorescence spectra of a dansyl monomer copolymerizable in aqueous media, Chem. Phys. Lett. 307 (1999) 55–61.
[28] R. Sarkar, M. Ghosh, S.K. Pal, Ultrafast relaxation dynamics of a biologically relevant probe dansyl at the micellar surface, J. Photochem. Photobiol. B: Biol. 78 (2005) 93–98.
[29] A. Fersht, Enzyme Structure and Mechanism, W.H. Freeman and Company, New York, 1985.
[30] D.V. O'Connor, D. Philips, Time Correlated Single Photon Counting, Academic Press, London, 1984.
[31] M.L. Horng, J.A. Gardecki, A. Papazyan, M. Maroncelli, Subpicosecond measurements of polar solvation dynamics: coumarin 153 revisited, J. Phys. Chem. 99 (1995) 17311–17337.
[32] A.S.R. Koti, M.M.G. Krishna, N. Periasamy, Time-resolved area-normalized emission spectroscopy (TRANES): a novel method for confirming emission from two excited states, J. Phys. Chem. A 105 (2001) 1767–1771.
[33] N. Spreti, F. Alfani, M. Cantarella, F. D'Amico, R. Germani, G. Savelli, α-chymotrypsin superactivity in aqueous solutions of cationic surfactants, J. Mol. Catal. B – Enzym. 6 (1999) 99–110.
[34] P. Viparelli, F. Alfani, M. Cantarella, Models for enzyme superactivity in aqueous solutions of surfactants, Biochem. J. 344 (1999) 765–773.
[35] O.G. Berg, M.H. Gelb, M.D. Tsai, M.K. Jain, Interfacial enzymology: the secreted phospholipase A_2-paradigm, Chem. Rev. 101 (2001) 2613–2653.
[36] P. Dutta, P. Sen, S. Mukherjee, K. Bhattacharyya, Solvation dynamics in DMPC vesicle in the presence of a protein, Chem. Phys. Lett. 382 (2003) 426–433.
[37] N.A. Smith, S.R. Meech, I.V. Rubtsov, K. Yoshihara, LDS-750 as a probe of solvation dynamics: a femtosecond time-resolved fluorescence study in liquid aniline, Chem. Phys. Lett. 303 (1999) 209–217.
[38] M. Viard, J. Gallay, M. Vincent, M. Paternostre, Origin of laurdan sensitivity to the vesicle-to-micelle transition of phospholipid–octylglucoside system: a time-resolved fluorescence study, Biophys. J. 80 (2001) 347–359.
[39] N. Nandi, K. Bhattacharyya, B. Bagchi, Dielectric relaxation and solvation dynamics of water in complex chemical and biological systems, Chem. Rev. 100 (2000) 2013–2045.